Research Square

Preprints are preliminary reports that have not undergone peer review.
They should not be considered conclusive, used to inform clinical practice,
or referenced by the media as validated information.

Effect of Laser Repetition Rate on the Physicochemical Properties and Antibacterial Activity of PVP-Stabilized CuO Nanoparticles

Ali Khumaeni

khumaeni@fisika.fsm.undip.ac.id

Diponegoro University

Citra Mayang Satriyani

Diponegoro University

Nafaul Mubarokah

Diponegoro University

Eko Hidayanto

Diponegoro University

Research Article

Keywords: copper oxide nanoparticles (CuO), pulsed laser ablation in liquid, laser repetition rate, polyvinylpyrrolidone, antibacterial activity, nanoparticle synthesis

Posted Date: November 12th, 2026

DOI: https://doi.org/10.21203/rs.3.rs-11558816/v1

License: This work is licensed under a Creative Commons Attribution 4.0 International License.
Read Full License

Additional Declarations: No competing interests reported.

Effect of Laser Repetition Rate on the Physicochemical Properties and Antibacterial Activity of PVP-Stabilized CuO Nanoparticles

Ali Khumaeni[1,2*], Citra Mayang Satriyani[1,2], Nafaul Mubarokah[1,2], and Eko Hidayanto[1]

[1] *Department of Physics, Faculty of Science and Mathematics, Diponegoro University, Tembalang, Semarang, 50275, Indonesia*

[2] *Research Centre for Laser and Advanced Nanotechnology, Faculty of Science and Mathematics, Diponegoro University, Tembalang, Semarang, 50275, Indonesia*

**Corresponding author: e-mail khumaeni@fisika.fsm.undip.ac.id*

Abstract

Copper oxide (CuO) nanoparticles are promising antibacterial materials due to their broad spectrum antimicrobial activity and low cost. The pulsed laser ablation in liquid (PLAL) technique provides a green and contamination free means for CuO nanoparticles synthesis. The laser repetition rate is an important parameter influencing the formation and yield of nanoparticles. In this study, the effect of laser repetition rate on physicochemical properties and antibacterial activity of CuO nanoparticles stabilized with polyvinylpyrrolidone (PVP) synthesized by PLAL was studied. CuO nanoparticles were prepared by laser ablation of a copper target in 5 mM PVP solution using a Nd:YAG laser (1064 nm, 30 mJ, 7 ns) at 10, 15 and 20 Hz repetition rates. The synthesized nanoparticles were characterized by UV–Vis spectroscopy, transmission electron microscopy (TEM) and Fourier transform infrared spectroscopy (FTIR). Antibacterial activity was determined by disk diffusion method against Staphylococcus aureus and Escherichia coli. The UV–Vis spectra showed the characteristic absorption peaks of CuO at 288–292 nm. With the increase in repetition rate, the absorbance intensity increased from 0.886 to 1.340 indicating the enhanced nanoparticle production. TEM analysis revealed average particle sizes of 5.70, 7.00 and 8.24 nm for the nanoparticles synthesized at repetition rates of 10, 15 and 20 Hz, respectively. The formation of CuO nanoparticles has been confirmed by FTIR analysis. The results of antibacterial test showed that the inhibition zone diameter increased from 1.30 to 3.10 mm against S. aureus and from 0.90 to 2.40 mm against E. coli with the increase of repetition rate from 10 to 20 Hz. The increase in antibacterial activity was attributed to the higher nanoparticle concentration produced at higher repetition rates . The laser repetition rate is a key factor affecting the antibacterial performance, particle size and nanoparticle yield of PVP-stabilized CuO nanoparticles fabricated by PLAL. Higher repetition rates showed increased nanoparticle

production and antibacterial activity suggesting that repetition rate is an effective parameter to tailor CuO nanoparticles for antimicrobial applications.

Keywords: copper oxide nanoparticles (CuO); pulsed laser ablation in liquid; laser repetition rate; polyvinylpyrrolidone; antibacterial activity; nanoparticle synthesis.

1. Introduction

The increasing prevalence of bacterial infections and the emergence of antibiotic-resistant microorganisms have become major global health concerns [1–3]. Conventional antibacterial agents are often associated with limited effectiveness against resistant bacterial strains, motivating the development of alternative antimicrobial materials [4]. Among various nanomaterials, metal oxide nanoparticles have attracted considerable attention because of their unique physicochemical properties and broad-spectrum antibacterial activity [5, 6]. Nanoparticles can interact directly with bacterial cell membranes, generate reactive oxygen species (ROS), and induce cellular damage, making them promising candidates for antimicrobial applications [7, 8].

Copper oxide (CuO) nanoparticles have emerged as attractive antibacterial materials due to their low cost, chemical stability, environmental compatibility, and strong antimicrobial performance against both Gram-positive and Gram-negative bacteria [9–11]. The antibacterial activity of CuO nanoparticles has been attributed to several mechanisms, including the generation of reactive oxygen species, release of Cu^{2+} ions, disruption of membrane integrity, and interference with intracellular biomolecules [12–14]. Previous studies have demonstrated that the antibacterial performance of CuO nanoparticles is strongly influenced by their physicochemical characteristics, particularly particle size, morphology, and concentration [15–17].

Various methods have been employed to synthesize CuO nanoparticles, including sol-gel, hydrothermal, precipitation, and chemical reduction techniques [18–20]. However, many of these methods require chemical reagents, reducing agents, or surfactants that may introduce impurities into the final products [21]. Pulsed Laser Ablation in Liquid (PLAL) has emerged as a promising alternative synthesis technique because it enables the production of high-purity

nanoparticles in liquid media without the need for additional chemical reducing agents [22–24]. During PLAL, a high-energy laser pulse interacts with a solid target immersed in a liquid medium, generating a plasma plume that subsequently cools and condenses into nanoparticles [25, 26].

Among the various synthesis parameters in PLAL, laser repetition rate plays a crucial role in determining nanoparticle formation and growth [27, 28]. Increasing the repetition rate increases the number of laser pulses delivered to the target per unit time, leading to enhanced material ablation and nanoparticle production [29]. However, the higher nanoparticle density generated at elevated repetition rates may also increase the probability of particle collisions and aggregation, thereby affecting particle size, colloidal stability, and other physicochemical properties [30, 31]. Previous studies have demonstrated that the characteristics of PLAL-synthesized nanoparticles are strongly influenced by laser processing parameters, including pulse energy, wavelength, ablation time, and liquid medium. Nevertheless, studies specifically investigating the influence of laser repetition rate on the physicochemical characteristics and antibacterial performance of CuO nanoparticles remain limited [32, 33]. In particular, the relationship between repetition-rate-induced changes in nanoparticle yield, particle size evolution, and antibacterial activity has not been comprehensively established. Furthermore, the use of polyvinylpyrrolidone (PVP) as a stabilizing medium may influence nanoparticle growth dynamics and colloidal stability, thereby affecting the resulting biological activity. Therefore, a systematic investigation of repetition rate effects is necessary to better understand and optimize the antibacterial performance of PLAL-synthesized CuO nanoparticles.

Therefore, this study aims to systematically investigate the effect of laser repetition rate on the physicochemical properties and antibacterial activity of polyvinylpyrrolidone (PVP)-stabilized CuO nanoparticles synthesized by PLAL. CuO nanoparticles were synthesized at repetition rates of 10, 15, and 20 Hz and characterized using UV–Vis spectroscopy, transmission electron microscopy (TEM), and Fourier transform infrared spectroscopy (FTIR). Their antibacterial activity against *Staphylococcus aureus* and *Escherichia coli* was evaluated using the disk diffusion method. The findings provide insight into the role of repetition rate in controlling nanoparticle formation and antibacterial performance, offering a simple strategy for tailoring CuO nanoparticles for antimicrobial applications.

2. Materials and Methods

2.1. Materials

A copper plate (Cu, 99.95% purity) was used as the ablation target for nanoparticle synthesis. Polyvinylpyrrolidone (PVP, 5 mM) was employed as a stabilizing agent and deionized water was used as the solvent. Nutrient agar and bacterial cultures of *Staphylococcus aureus* and *Escherichia coli* were used for antibacterial activity evaluation.

2.2. Synthesis of CuO Nanoparticles by Pulsed Laser Ablation in Liquid

CuO nanoparticles were synthesized using the Pulsed Laser Ablation in Liquid (PLAL) method. The copper target was placed at the bottom of a glass vessel containing 10 mL of 5 mM PVP solution. A Q-switched Nd:YAG laser operating at a wavelength of 1064 nm, pulse energy of 30 mJ, and pulse duration of 7 ns was focused onto the target surface using a convex lens.

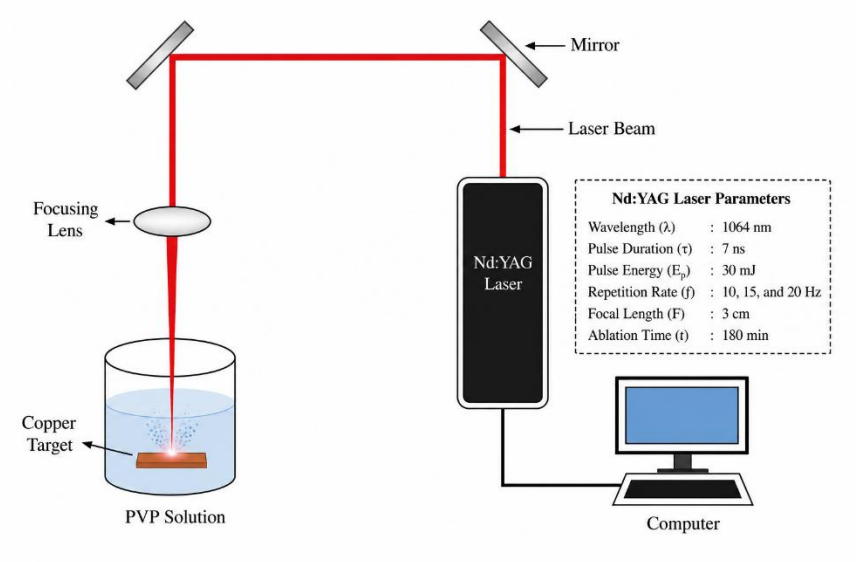


Figure 1. Schematic illustration of CuO nanoparticle synthesis by pulsed laser ablation in liquid.

The synthesis was performed at repetition rates of 10, 15, and 20 Hz while maintaining identical experimental conditions. The ablation process was conducted for 180 min to obtain CuO nanoparticle colloids. During laser irradiation, the interaction between the laser pulses and the

copper target generated a plasma plume, followed by rapid cooling and condensation in the liquid medium, resulting in the formation of CuO nanoparticles stabilized by PVP.

2.3. Characterization of CuO Nanoparticles

The optical properties of the synthesized CuO nanoparticles were investigated using UV–Vis spectroscopy in the wavelength range of 200–500 nm. The morphology and particle size distribution of the nanoparticles were analyzed using transmission electron microscopy (TEM). The particle size distribution was estimated from the TEM micrographs by measuring individual nanoparticles and constructing size distribution histograms. Fourier transform infrared spectroscopy (FTIR) was performed on a representative CuO nanoparticle sample to identify the functional groups present and to confirm the formation of Cu–O bonds.

2.4. Antibacterial Activity Test

The synthesized CuO nanoparticles were evaluated for antibacterial activity against Gram-positive Staphylococcus aureus and Gram-negative Escherichia coli by disk diffusion method. The bacterial suspensions were adjusted to turbidity equal to a 0.5 McFarland standard (≈1.5×10^8 CFU mL-1). Sterile paper disks of 6 mm in diameter were immersed in CuO nanoparticle colloids synthesized with repetition rates of 10, 15 and 20 Hz. The disks were then placed on agar plates inoculated with bacterial cultures and incubated for 48 h at 37 °C. A commercial antibacterial liquid soap containing silver nanoparticles was used as a positive control and a 5 mM PVP solution without CuO nanoparticles was used as a negative control. The antibacterial activity was assessed by measuring the diameter of inhibition zone formed around each disk after incubation.

3. Results and Discussion

3.1. Visual Observation of CuO Nanoparticle Colloids

Figure 1 presents the appearance of CuO nanoparticle colloids synthesized in a 5 mM PVP solution at laser repetition rates of 10, 15, and 20 Hz. All colloidal samples exhibited a pale yellow coloration, indicating the successful formation of CuO nanoparticles in the liquid medium. No visible sedimentation or phase separation was observed immediately after synthesis, demonstrating the effectiveness of PVP in stabilizing the nanoparticle dispersion.

As shown in Figure 1, the color intensity of the colloidal suspension increased with increasing repetition rate. The sample synthesized at 20 Hz exhibited the darkest yellow coloration, followed by the samples synthesized at 15 Hz and 10 Hz. This observation suggests that a higher repetition rate promotes greater material ablation from the copper target, resulting in a larger quantity of nanoparticles dispersed in the solution.



(a) (b) (c)

Figure 2. CuO nanoparticle colloids prepared by PVP 20 Hz (a), 15 Hz (b), and 10 Hz (c)

The increased nanoparticle concentration at higher repetition rates can be attributed to the greater number of laser pulses delivered to the target per unit time. More frequent laser-target interactions enhance plasma generation and material removal, thereby increasing nanoparticle production during the PLAL process. The enhanced antibacterial activity at higher repetition rates is consistent with the increased absorbance intensity observed in the UV–Vis spectra, indicating a higher concentration of CuO nanoparticles available to interact with bacterial cells.

3.2. UV–Vis Absorption Analysis

The optical properties of the synthesized CuO nanoparticles were investigated using UV–Vis spectroscopy, and the obtained absorption spectra are presented in Figure 2. All samples exhibited a prominent absorption peak within the wavelength range of 288–292 nm, which is commonly attributed to CuO nanoparticles. The absorption maximum was observed at approximately 288 nm for the sample synthesized at 10 Hz, whereas the samples synthesized at 15 Hz and 20 Hz exhibited absorption maxima at around 292 nm.

As shown in Figure 2, the absorbance intensity increased significantly with increasing laser repetition rate. The maximum absorbance values were 0.886, 1.180, and 1.340 for the samples synthesized at repetition rates of 10, 15, and 20 Hz, respectively. The increase in absorbance intensity indicates a higher concentration of CuO nanoparticles in the colloidal suspension. This phenomenon can be attributed to the greater number of laser pulses delivered to the copper target per unit time at higher repetition rates, resulting in enhanced ablation efficiency and increased nanoparticle production.

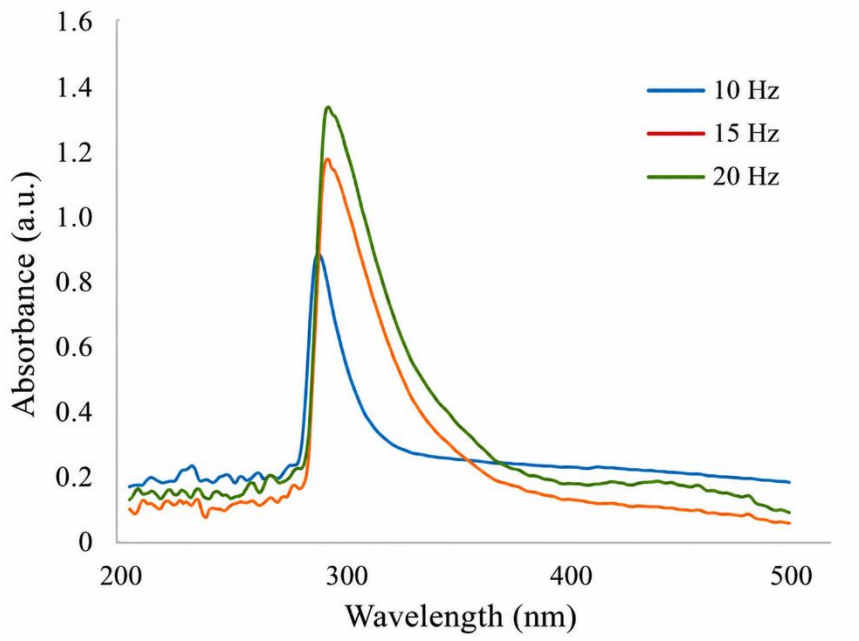


Figure 3. UV-Vis absorption spectrum of CuO nanoparticles at various laser repetition rates

The slight shift of the absorption peak from 288 nm to 292 nm may be associated with changes in particle size and nanoparticle concentration induced by variations in repetition rate. Similar behavior has been reported in PLAL-synthesized metal oxide nanoparticles, where laser processing parameters influence the optical response through modifications in particle growth dynamics and colloidal characteristics.

Furthermore, the UV–Vis results are consistent with the visual observations shown in Figure 1. The darker yellow coloration observed in the colloid synthesized at 20 Hz corresponds to its higher absorbance intensity, indicating a greater nanoparticle yield compared to the samples synthesized at 10 Hz and 15 Hz. These findings demonstrate that laser repetition rate plays an important role in controlling the production of CuO nanoparticles during the PLAL process.

3.3. Morphological Analysis of CuO Nanoparticles

The morphology of the synthesized CuO nanoparticles was examined using transmission electron microscopy (TEM), and the corresponding micrographs are presented in Figure 3. The TEM images confirm the successful formation of CuO nanoparticles at all investigated repetition rates. The nanoparticles appear as dark contrast regions dispersed within a lighter background, indicating the presence of Cu-containing nanostructures embedded in the PVP matrix.

As shown in Figure 3(a–c), the synthesized nanoparticles exhibit irregularly shaped nanostructures with a tendency to form aggregates. Such aggregation is commonly observed in PLAL-synthesized nanoparticles due to their high surface energy and frequent interparticle interactions during particle growth. Despite the presence of PVP as a stabilizing agent, partial agglomeration can still occur during nanoparticle formation and subsequent drying of the TEM samples.

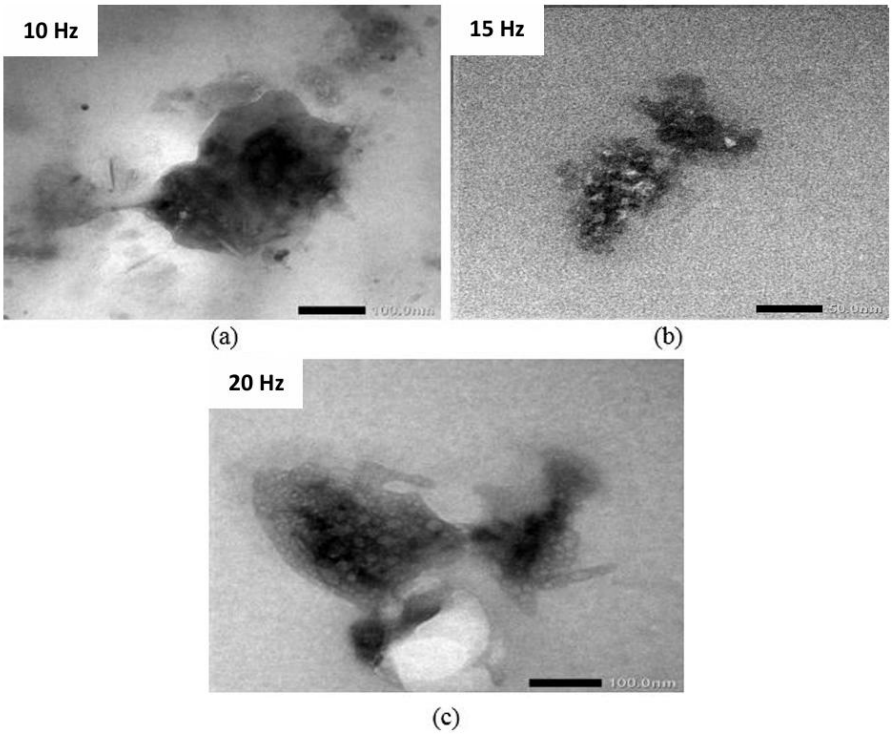


Figure 4. TEM images of CuO nanoparticles 10 Hz (a), 15 Hz (b), and 20 Hz (c).

A noticeable difference in particle assembly can be observed as the repetition rate increases. The nanoparticles synthesized at 10 Hz exhibit relatively smaller aggregates, whereas larger and denser particle clusters are observed in the samples synthesized at 15 Hz and 20 Hz. This

behavior suggests that increasing the repetition rate enhances nanoparticle production, leading to a higher probability of particle collision and aggregation within the colloidal suspension.

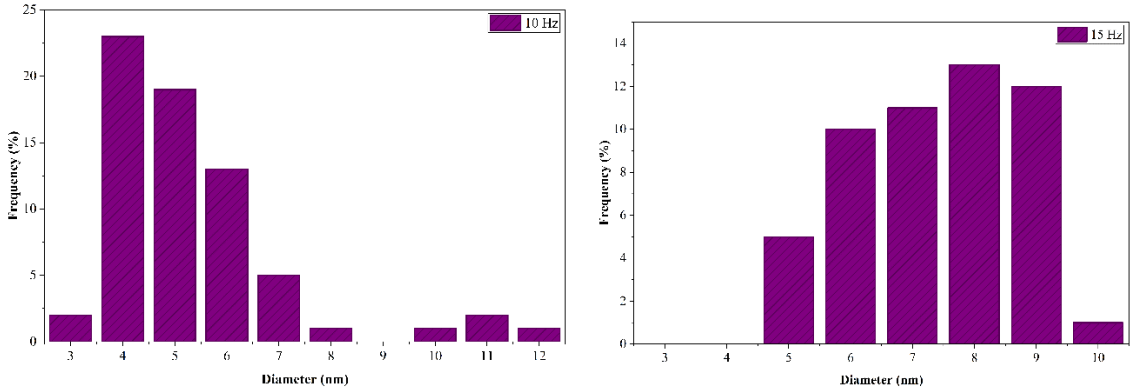
The morphological observations indicate that laser repetition rate influences not only nanoparticle yield but also the growth and aggregation behavior of CuO nanoparticles during the PLAL process. A more detailed quantitative analysis of particle size distribution is discussed in the following section.

3.4. Particle Size Distribution

The particle size distribution of the synthesized CuO nanoparticles was estimated from the TEM micrographs, and the corresponding histograms are presented in Figure 4. The average particle sizes were determined to be 5.70 nm, 7.00 nm, and 8.24 nm for the samples synthesized at repetition rates of 10, 15, and 20 Hz, respectively.

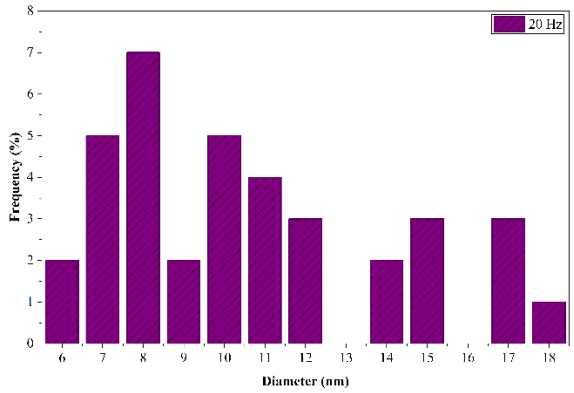
As shown in Figure 4, the particle size distribution gradually shifted toward larger diameters with increasing repetition rate. The CuO nanoparticles synthesized at 10 Hz exhibited a relatively narrow size distribution dominated by particles below 7 nm. In contrast, the samples synthesized at 15 Hz and 20 Hz displayed broader size distributions and slightly larger average particle diameters. At higher repetition rates, the interval between successive laser pulses becomes shorter, increasing the nanoparticle concentration within the ablation zone. This condition enhances particle–particle interactions and coalescence, resulting in gradual particle growth and broader size distributions.

The increase in particle size with repetition rate can be attributed to the higher density of nanoparticles generated during the PLAL process. At elevated repetition rates, laser pulses are delivered more frequently to the target surface, producing a greater amount of ablated material within the liquid medium. The resulting increase in nanoparticle concentration enhances the probability of particle collisions and coalescence, leading to gradual particle growth.



(a)

(b)



(c)

Figure 5. Particle size distribution histograms of CuO nanoparticles 10 Hz (a), 15 Hz (b), and 20 Hz (c).

In addition, the shorter interval between consecutive laser pulses at higher repetition rates may influence plasma evolution and nanoparticle growth dynamics. The accumulation of nanoparticles in the ablation zone can promote secondary interactions among particles, thereby contributing to the observed increase in particle size. Similar trends have been reported in PLAL-based synthesis, where increasing repetition rate enhances nanoparticle production while simultaneously promoting particle growth.

Despite the increase in average particle size, all synthesized CuO nanoparticles remained within the nanometer scale (<10 nm), indicating that the PLAL method combined with PVP stabilization is effective for producing ultrafine CuO nanoparticles. The particle size evolution

observed in Figure 4 is consistent with the TEM images presented in Figure 3, which show a gradual increase in aggregate size as the repetition rate increased from 10 Hz to 20 Hz.

3.5. FTIR Analysis

FTIR analysis was performed on a representative CuO nanoparticle sample synthesized in PVP solution to identify the functional groups and confirm Cu-O bond formation. As shown in Figure 5, a broad absorption band was observed in the region of 3260–3540 cm^{-1}, which is attributed to O–H stretching vibrations originating from adsorbed water molecules and surface hydroxyl groups. The presence of hydroxyl groups is commonly observed in metal oxide nanoparticles synthesized in aqueous environments and contributes to their surface reactivity.

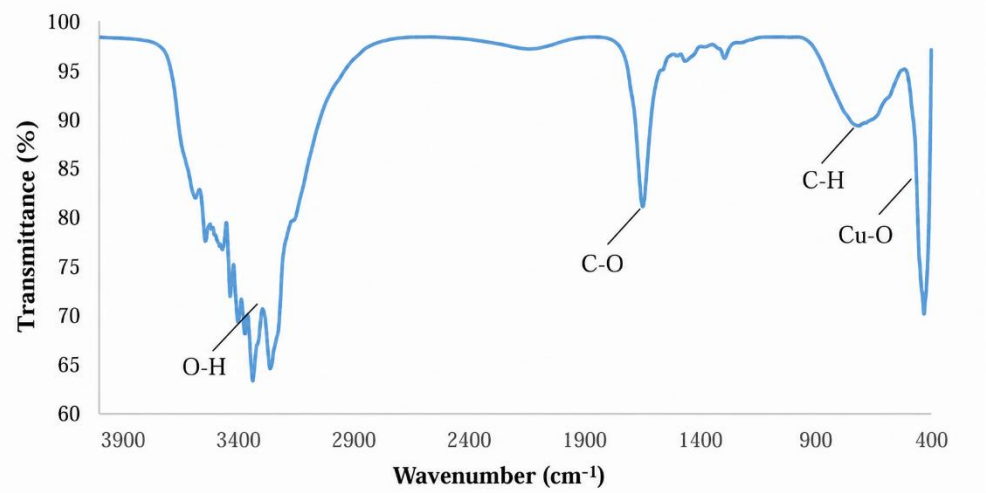


Figure 6. FTIR spectrum of CuO nanoparticles

A distinct absorption band at approximately 1649 cm^{-1} corresponds to C=O stretching vibrations, which may be associated with residual organic species from the PVP stabilizer. The absorption band observed around 1400–1500 cm^{-1} can be assigned to C–O related vibrations, indicating interactions between the nanoparticle surface and stabilizing molecules.

In the lower wavenumber region, characteristic absorption bands were observed at approximately 712 cm^{-1} and 431 cm^{-1}. These bands are attributed to Cu–O stretching vibrations and are considered characteristic fingerprints of copper oxide nanoparticles. The presence of these bands confirms the successful formation of CuO during the PLAL process.

Overall, the FTIR analysis verifies the existence of hydroxyl groups, residual PVP-related functional groups, and Cu–O bonds, supporting the successful synthesis of CuO nanoparticles in the PVP medium.

3.6. Antibacterial Activity

The antibacterial activity of the synthesized CuO nanoparticles was evaluated against Gram-positive *Staphylococcus aureus* and Gram-negative *Escherichia coli* using the disk diffusion method. Figure 7 shows the bacterial culture media before incubation, whereas Figure 8 presents the inhibition zones formed after 48 h of incubation. The corresponding inhibition zone diameters are summarized in Table 1.

As shown in Figure 8 and Table 1, the synthesized CuO nanoparticles exhibited antibacterial activity against both bacterial strains. For *S. aureus*, the inhibition zone diameter increased from 1.30 mm at 10 Hz to 2.05 mm at 15 Hz and reached 3.10 mm at 20 Hz. Similarly, for *E. coli*, the inhibition zone diameter increased from 0.90 mm to 1.60 mm and 2.40 mm with increasing repetition rate. These results indicate that higher repetition rates enhance the antibacterial performance of the synthesized CuO nanoparticles.

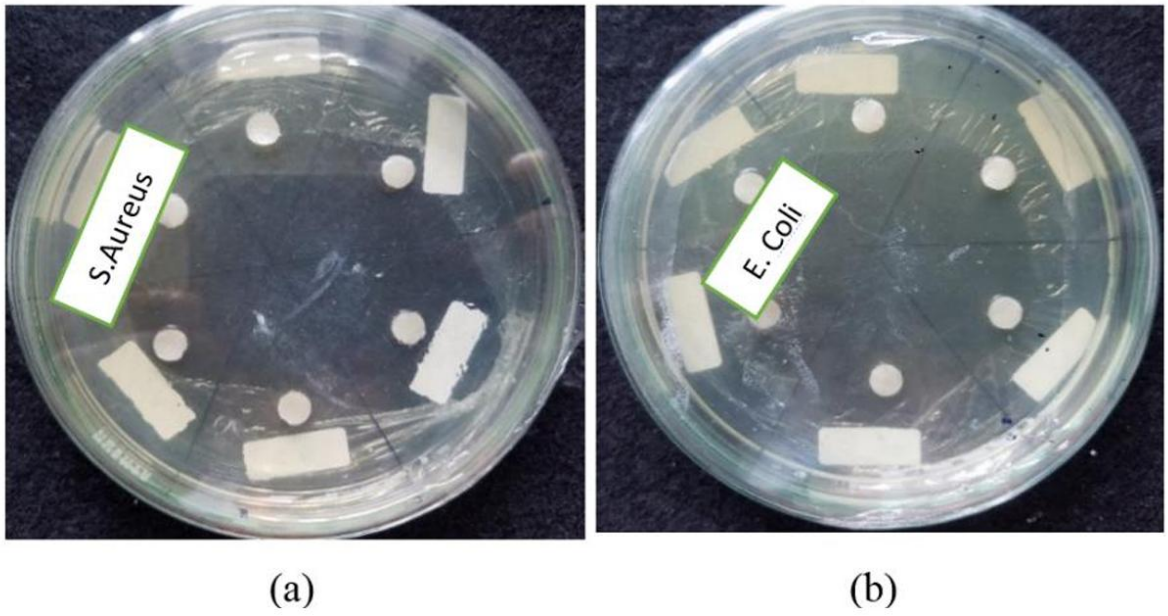


Figure 7. Antibacterial disc diffusion assays against *S. aureus* (a), *E. coli* (b).

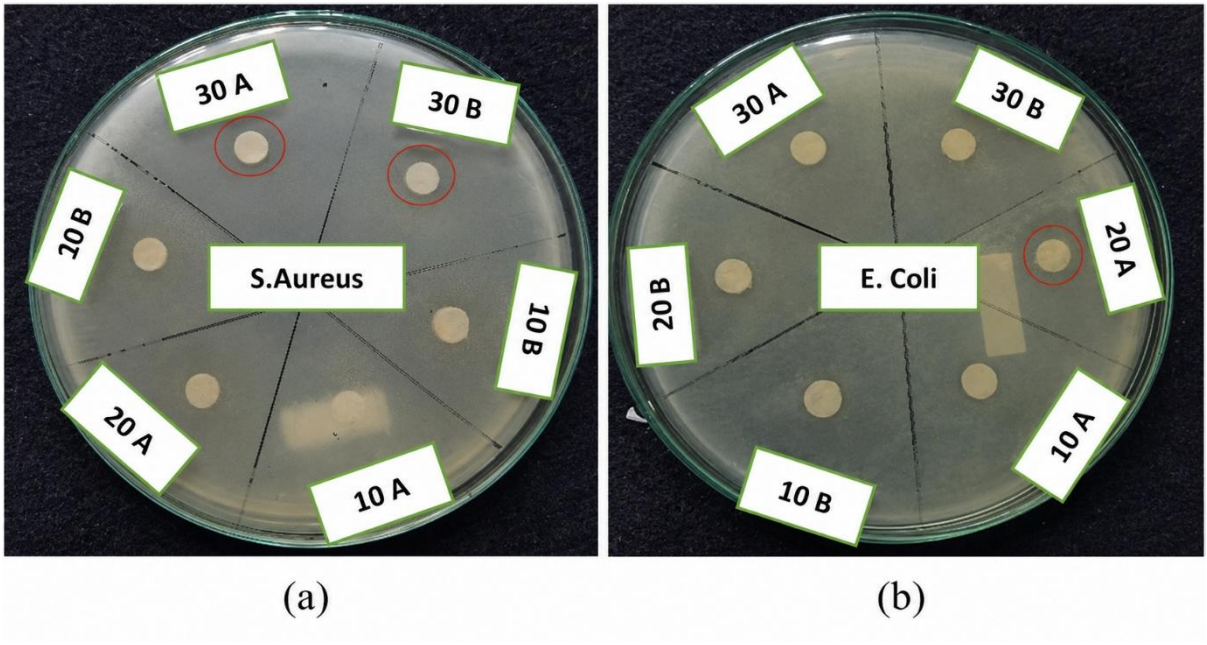


Figure 8. Antibacterial activity of CuO nanoparticles against *S. aureus* (a), *E. coli* (b).

Table 1

Inhibition zone diameters against S. aureus and E. coli.

Sample Name	DIZ (mm)	Methods
Positive control	4.80	Disc (Staphylococcus Aureus)
Negative control	Resistance	
10 Hz	1.30	
15 Hz	2.05	
20 Hz	3,10	
Positive control	5.00	Disc (Escherichia Coli)
Negative control	1.10	
10 Hz	0.90	
15 Hz	1.60	
20 Hz	2.40	

The observed trend is consistent with the UV–Vis results, which showed increased absorbance intensity with increasing repetition rate. Higher repetition rates generate a larger number of laser pulses per unit time, resulting in greater material ablation and higher nanoparticle production. Consequently, the increased concentration of CuO nanoparticles in the colloidal suspension enhances their interaction with bacterial cells, leading to larger inhibition zones.

The positive controls exhibited inhibition zone diameters of 4.80 mm and 5.00 mm against *S. aureus* and *E. coli*, respectively, confirming the effectiveness of the antibacterial assay. In contrast, the negative control showed no inhibition against *S. aureus* and only a very small inhibition zone of 1.10 mm against *E. coli*. These findings indicate that the antibacterial activity primarily originated from the synthesized CuO nanoparticles rather than the stabilizing medium.

Furthermore, the inhibition zones observed for *S. aureus* were consistently larger than those for *E. coli*. This difference can be attributed to variations in bacterial cell wall structure. Gram-negative bacteria such as *E. coli* possess an additional outer membrane composed of lipopolysaccharides, which acts as a protective barrier against external antimicrobial agents. In contrast, Gram-positive bacteria such as *S. aureus* lack this outer membrane, making them more susceptible to CuO nanoparticle-induced damage.

A schematic illustration of the proposed antibacterial mechanism of CuO nanoparticles is presented in Figure 9. The antibacterial activity of CuO nanoparticles is generally attributed to multiple synergistic mechanisms, including membrane disruption, Cu^{2+} ion release, and reactive oxygen species (ROS) generation. Initially, CuO nanoparticles interact with the bacterial cell surface and disrupt membrane integrity, resulting in increased membrane permeability and leakage of intracellular components. Simultaneously, Cu^{2+} ions released from the nanoparticle surface can penetrate the cell and interact with intracellular biomolecules, causing protein denaturation, enzyme deactivation, and DNA damage.

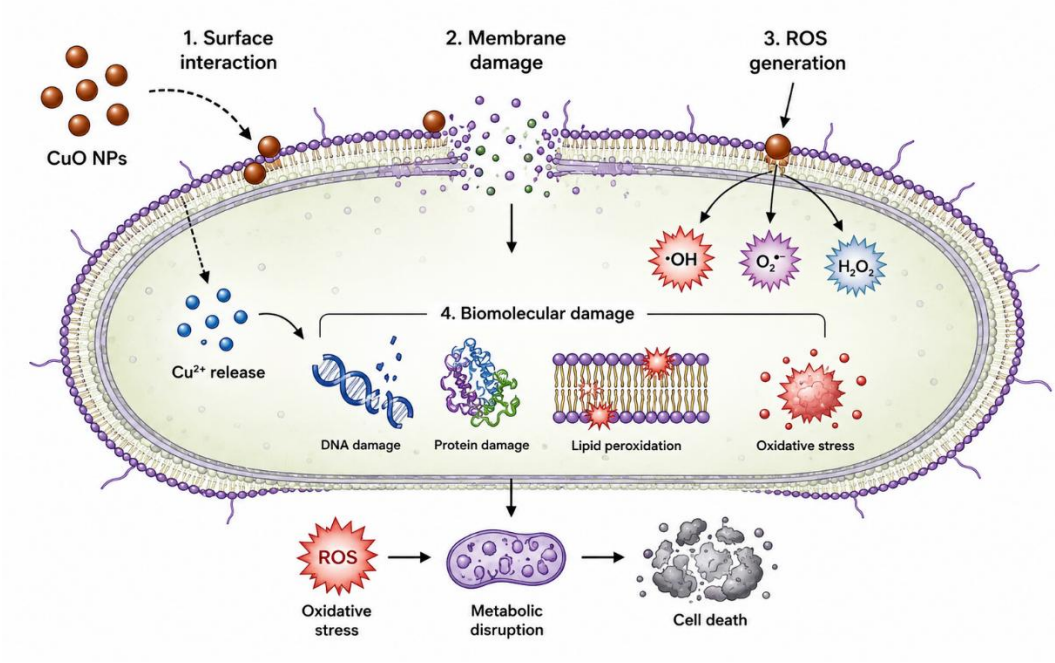


Figure 9. Antibacterial mechanism of CuO nanoparticles

In addition, CuO nanoparticles promote the formation of ROS, including hydroxyl radicals (•OH), superoxide radicals ($O_2^{\bullet-}$), and hydrogen peroxide (H_2O_2). Excessive ROS production induces oxidative stress, leading to lipid peroxidation, protein oxidation, and nucleic acid damage. The combined effects of membrane disruption, Cu^{2+} ion release, and ROS generation ultimately result in irreversible cellular damage and bacterial cell death.

Overall, the results demonstrate that increasing laser repetition rate enhances the antibacterial performance of PLAL-synthesized CuO nanoparticles. The higher nanoparticle yield produced at elevated repetition rates provides more active sites for bacterial interaction and promotes stronger antibacterial effects, with the highest activity observed for the sample synthesized at 20 Hz.

4. Conclusions

CuO nanoparticles were successfully synthesized in a 5 mM PVP solution using the Pulsed Laser Ablation in Liquid (PLAL) method with repetition rates of 10, 15, and 20 Hz. The repetition rate significantly influenced the physicochemical characteristics of the synthesized nanoparticles. UV–Vis analysis showed that increasing the repetition rate enhanced the absorbance intensity, indicating a higher nanoparticle yield. TEM observations confirmed the average particle size increased from 5.70 nm to 8.24 nm as the repetition rate increased from

10 Hz to 20 Hz. FTIR analysis further verified the formation of CuO nanoparticles. The synthesized CuO nanoparticles exhibited antibacterial activity against both *Staphylococcus aureus* and *Escherichia coli*. The inhibition zone diameter increased with increasing repetition rate, reaching the highest values for nanoparticles synthesized at 20 Hz. This enhancement was attributed to the greater nanoparticle concentration generated at higher repetition rates, which increased the interaction between CuO nanoparticles and bacterial cells. These findings demonstrate that laser repetition rate is a key parameter for tailoring the physicochemical properties and antibacterial performance of PLAL-synthesized CuO nanoparticles, highlighting the potential of PLAL as a simple and environmentally friendly approach for producing antibacterial CuO nanoparticles with tunable properties.

Author Contributions

A.K.: conceptualization, methodology, investigation, data curation, writing an original draft, funding acquisition; C.M.S.: investigation, data curation, visualization, writing an original draft; N.M.: investigation, data analysis, validation, writing—reviewing and editing; E.H.: conceptualization, supervision, resources writing—reviewing and editing; All authors have read and agreed to the published version of the manuscript.

Declaration of generative AI in scientific writing

During the preparation of this work, the authors used OpenAI to improve the language, grammar, and readibility of the manuscript. After using this tool, the authors carefully reviewed and edited the content and take full responsibility for the content of the publication.

Declaration of Competing Interest

The authors declare that they have no known competing financial interests or personal relationships that could have appeared to influence the work reported in this paper.

Acknowledgments

This work was financially supported by the Faculty of Science and Mathematics, Universitas Diponegoro, through the Research Assignment Program 2026 (Dean's Decree No. 161/UN7.F8/HK/III/2026; Research Contract No. 450.B/UN7.F8/PP/III/2026).

References

1. Shoudho, K. N., Uddin, S., Rumon, M. M. H., & Shakil, M. S. (2024). Influence of physicochemical properties of iron oxide nanoparticles on their antibacterial activity. *ACS omega*, *9*(31), 33303-33334. https://doi.org/10.1021/acsomega.4c02822.
2. Ijaz, I., Bukhari, A., Gilani, E., Nazir, A., Zain, H., & Saeed, R. (2022). Green synthesis of silver nanoparticles using different plants parts and biological organisms, characterization and antibacterial activity. *Environmental Nanotechnology, Monitoring & Management*, *18*, 100704. https://doi.org/10.1016/j.enmm.2022.100704.
3. Jawad, M. H., & Abdulameer, M. R. (2026). Eco-friendly laser ablation for synthesis of Al-Ni nanoparticles: insights into enhancing glucose biosensor performance and antibacterial activity. *Lasers in Manufacturing and Materials Processing*, *13*(1), 1-22. https://doi.org/10.1007/s40516-025-00322-8.
4. Nahar, B., Chaity, S. B., Gafur, M. A., & Hossain, M. Z. (2023). Synthesis of spherical copper oxide nanoparticles by chemical precipitation method and investigation of their photocatalytic and antibacterial activities. *Journal of Nanomaterials*, *2023*(1), 2892081. https://doi.org/10.1155/2023/2892081.
5. Hatami, K. K., Baghbantaraghdari, Z., Jamaledin, D., Dabbagh, M. F., Kaneko, N., & Ghovvati, M. (2023). Synthesis, characterization, antioxidant and antibacterial activities of zinc ferrite and copper ferrite nanoparticles. https://doi.org/10.22128/MCH.2022.613.1030.
6. Franco, D., Calabrese, G., Guglielmino, S. P. P., & Conoci, S. (2022). Metal-based nanoparticles: antibacterial mechanisms and biomedical application. *Microorganisms*, *10*(9), 1778. https://doi.org/10.3390/microorganisms10091778.
7. Alavi, M., Hamblin, M. R., Martinez, F., Kennedy, J. F., & Khan, H. (2022). Synergistic combinations of metal, metal oxide, or metalloid nanoparticles plus antibiotics against resistant and non-resistant bacteria. *Micro Nano Bio Aspects*, *1*(1), 1-9.
8. Ghazzy, A., Naik, R. R., & Shakya, A. K. (2023). Metal–polymer nanocomposites: A promising approach to antibacterial materials. *Polymers*, *15*(9), 2167. https://doi.org/10.3390/polym15092167.
9. Goncalves, R. A., Ku, J. W., Zhang, H., Salim, T., Oo, G., Zinn, A. A., ... & Lam, Y. M. (2022). Copper-nanoparticle-coated fabrics for rapid and sustained antibacterial activity

applications. *ACS Applied Nano Materials*, *5*(9), 12876-12886. https://doi.org/10.1021/acsanm.2c02736.

10. Nieto-Maldonado, A., Bustos-Guadarrama, S., Espinoza-Gomez, H., Flores-López, L. Z., Ramirez-Acosta, K., Alonso-Nuñez, G., & Cadena-Nava, R. D. (2022). Green synthesis of copper nanoparticles using different plant extracts and their antibacterial activity. *Journal of Environmental Chemical Engineering*, *10*(2), 107130. https://doi.org/10.1016/j.jece.2022.107130.
11. Sharma, P., Goyal, D., & Chudasama, B. (2022). Antibacterial activity of colloidal copper nanoparticles against Gram-negative (Escherichia coli and Proteus vulgaris) bacteria. *Letters in applied microbiology*, *74*(5), 695-706. https://doi.org/10.1111/lam.13655.
12. Khatoon, U. T., Velidandi, A., & Rao, G. N. (2023). Copper oxide nanoparticles: synthesis via chemical reduction, characterization, antibacterial activity, and possible mechanism involved. *Inorganic Chemistry Communications*, *149*, 110372. https://doi.org/10.1016/j.inoche.2022.110372.
13. Jabeen, S., Siddiqui, V. U., Bala, S., Mishra, N., Mishra, A., Lawrence, R., ... & Khan, T. (2024). Biogenic synthesis of copper oxide nanoparticles from aloe vera: Antibacterial activity, molecular docking, and photocatalytic dye degradation. *ACS omega*, *9*(28), 30190-30204. https://doi.org/10.1021/acsomega.3c10179.
14. Taghavi, F. S., Moradnia, F., & Heidarzadeh, S. (2023). Green synthesis, characterization, photocatalytic and antibacterial activities of copper oxide nanoparticles. https://doi.org/10.22036/ncr.2023.02.006.
15. Hassan, E., Gahlan, A. A., & Gouda, G. A. (2023). Biosynthesis approach of copper nanoparticles, physicochemical characterization, cefixime wastewater treatment, and antibacterial activities. *BMC chemistry*, *17*(1), 71. https://doi.org/10.1186/s13065-023-00982-7.
16. Gao, J., Lu, H., Yin, H., Zou, G., Chen, X., Jiang, T., ... & Wang, Y. (2025). Enhanced antibacterial activity through photothermal therapy of copper nanoparticles on titanium-based implants. *Materialia*, 102514. https://doi.org/10.1016/j.mtla.2025.102514.
17. Lai, M. J., Huang, Y. W., Chen, H. C., Tsao, L. I., Chang Chien, C. F., Singh, B., & Liu, B. R. (2022). Effect of size and concentration of copper nanoparticles on the antimicrobial activity in Escherichia coli through multiple mechanisms. *Nanomaterials*, *12*(21), 3715. https://doi.org/10.3390/nano12213715.

18. Johnson, E., Krishnan, R. R., Chandran, S. R., & Prema, K. H. (2023). Green mediated sol-gel synthesis of copper oxide nanoparticle: An efficient candidate for waste water treatment and antibacterial agent. *Journal of Sol-Gel Science and Technology*, *107*(3), 697-710. https://doi.org/10.1007/s10971-023-06172-0.
19. Abaas, R., Salim, E., & Mahdi, R. (2023). A sight of view on hydrothermal synthesis of copper oxide. *Engineering and Technology Journal*, *41*(4), 592-602. https://doi.org/10.30684/etj.2023.138424.1391.
20. Nahar, B., Chaity, S. B., Gafur, M. A., & Hossain, M. Z. (2023). Synthesis of spherical copper oxide nanoparticles by chemical precipitation method and investigation of their photocatalytic and antibacterial activities. *Journal of Nanomaterials*, *2023*(1), 2892081. https://doi.org/10.1155/2023/2892081.
21. Chakraborty, N., Banerjee, J., Chakraborty, P., Banerjee, A., Chanda, S., Ray, K., ... & Sarkar, J. (2022). Green synthesis of copper/copper oxide nanoparticles and their applications: a review. *Green Chemistry Letters and Reviews*, *15*(1), 187-215. https://doi.org/10.1080/17518253.2022.2025916.
22. Khairani, I. Y., Mínguez-Vega, G., Doñate-Buendía, C., & Gökce, B. (2023). Green nanoparticle synthesis at scale: a perspective on overcoming the limits of pulsed laser ablation in liquids for high-throughput production. *Physical Chemistry Chemical Physics*, *25*(29), 19380-19408. https://doi.org/10.1039/D3CP01214J.
23. Mehta, K., & Baruah, P. K. (2022). A comprehensive review and outlook on the experimental techniques to investigate the complex dynamics of pulsed laser ablation in liquid for nanoparticle synthesis. *Review of Scientific Instruments*, *93*(9). https://doi.org/10.1063/5.0084803.
24. Subhan, A., Mourad, A. H. I., & Al-Douri, Y. (2022). Influence of laser process parameters, liquid medium, and external field on the synthesis of colloidal metal nanoparticles using pulsed laser ablation in liquid: a review. *Nanomaterials*, *12*(13), 2144. https://doi.org/10.3390/nano12132144.
25. Ahmed, A. M., Halim, M. M., Ahmed, N. M., Rashid, M., & Taha, B. A. (2025). Advances in pulsed laser ablation in liquid for silver and copper synthesis: from plasma generation to nanoparticle formation. *physica status solidi (a)*, *222*(18), 2500382. https://doi.org/10.1002/pssa.202500382.
26. AlMalki, F. A., Khashan, K. S., Jabir, M. S., Hadi, A. A., Sulaiman, G. M., Abdulameer, F. A., ... & Albaqami, J. (2022). Eco-friendly synthesis of carbon nanoparticles by laser

ablation in water and evaluation of their antibacterial activity. *Journal of Nanomaterials*, *2022*(1), 7927447. https://doi.org/10.1155/2022/7927447.

27. Attallah, A. H., Abdulwahid, F. S., Ali, Y. A., & Haider, A. J. (2023). Effect of liquid and laser parameters on fabrication of nanoparticles via pulsed laser ablation in liquid with their applications: a review. *Plasmonics*, *18*(4), 1307-1323. https://doi.org/10.1007/s11468-023-01852-7.
28. Jia, X., & Zhao, X. (2023). Ultrafast laser ablation of copper with GHz bursts: A numerical study on the effects of repetition rate, pulse number and burst fluence on ablation efficiency and heat-affected zone. *Optics & Laser Technology*, *158*, 108803. https://doi.org/10.1016/j.optlastec.2022.108803.
29. Igarashi, K., Iwasa, M., Sasaki, T., Takahashi, K., & Kikuchi, T. (2022). Performance of laser ablation propulsion with a high-repetition rate and high-power laser. *AIP Advances*, *12*(2). https://doi.org/10.1063/5.0082109.
30. Govindassamy, G. A., Prentice, J. J., Lunney, J. G., Eason, R. W., & Mackenzie, J. I. (2022). Effect of laser repetition rate on the growth of Sc2O3 via pulsed laser deposition. *Applied Physics A*, *128*(7), 577. https://doi.org/10.1007/s00339-022-05698-4.
31. Al-Senani, G. M., Alrefaee, S. H., Al-Ahmadi, A. N., ElFaham, M. M., Almotairy, A. R. Z., Elsharkawy, W. B., & Mostafa, A. M. (2023). Effect of laser pulse repetition rate in the synthesis of nickel oxide nanoparticles in PVA solution on the adsorption efficiency against phosphate ions. *Radiation Physics and Chemistry*, *208*, 110872. https://doi.org/10.1016/j.radphyschem.2023.110872.
32. Hesabizadeh, T., Sung, K., Park, M., Foley, S., Paredes, A., Blissett, S., & Guisbiers, G. (2023). Synthesis of antibacterial copper oxide nanoparticles by pulsed laser ablation in liquids: potential application against foodborne pathogens. *Nanomaterials*, *13*(15), 2206. https://doi.org/10.3390/nano13152206.
33. Qona'ah, A., Suliyanti, M. M., Hidayanto, E., & Khumaeni, A. (2023). Characteristics of copper oxide and tin oxide nanoparticles produced by using pulsed laser ablation method and their application as an antibacterial agent. *Results in Chemistry*, *6*, 101042. https://doi.org/10.1016/j.rechem.2023.101042.